

Micro/Miniature Aerial Vehicle Guidance for Hurricane Research

Doug Lipinski and Kamran Mohseni, *Member, IEEE*

Abstract—We present an investigation of the Lagrangian dynamics of a hurricane from the perspective of using micro aerial vehicles (MAVs) or small unmanned aircraft systems as mobile sensors for hurricane research and monitoring. The low cost of MAVs allows the use of more sensors for volumetric *in situ* measurements, particularly in high-risk locations where larger more expensive systems cannot be used. However, the limited flight speed of MAVs enforces severe restrictions on potential flight plans. In the face of 70-m/s horizontal winds, a MAV with only 10-m/s flight capability has very little directional control. Fortunately, vertical wind speeds in the hurricane are much lower and have limited spatial extent. Using Lagrangian coherent structure techniques and simplified vehicle simulations, we develop an understanding of the transport dynamics of a simulated hurricane and apply this understanding to a high-level control scheme to enable MAV navigation and guidance near the hurricane. By smartly adjusting their altitude, simulated MAVs are able to navigate into the hurricane eye at a very high success rate. Our findings suggest that the smart use of the existing background flow could allow the use of low-cost sensor platforms in extreme environments.

Index Terms—Environmental monitoring, hurricanes, path planning, unmanned aerial vehicles.

I. INTRODUCTION

DESPITE the enormous impact and cost associated with hurricanes, the past few decades have seen relatively little progress in the area of *in situ* hurricane measurement and monitoring. The state of the art for *in situ* data collection prior to landfall currently consists of large aircraft reconnaissance flights [1], dropsonde deployment [2]–[4], or some larger unmanned aerial vehicles. Recent efforts to develop micro aerial vehicles (MAVs) and small unmanned aircraft systems (sUAS) have led to many breakthroughs that may soon allow their use in hurricane research and data collection. MAVs such as those shown in Fig. 1 are small light very low cost easily deployed multiuse vehicles that may allow for completely new methods of data collection using large swarms of cheap vehicles [5]. Dozens or even hundreds of MAVs could be released for the

Manuscript received November 15, 2014; revised May 20, 2015 and August 26, 2015; accepted September 5, 2015. This paper has supplementary downloadable material available at <http://ieeexplore.ieee.org>, provided by the authors.

D. Lipinski was with the Department of Mechanical and Aerospace Engineering, University of Florida at Gainesville, Gainesville, FL 32603 USA. He is now with Massachusetts Institute of Technology Lincoln Laboratory, Lexington, MA 02420-9108 USA.

K. Mohseni is with the Institute for Networked Autonomous Systems, Department of Mechanical and Aerospace Engineering, University of Florida, Gainesville, FL 32611 USA, and also with the Department of Electrical and Computer Engineering, University of Florida, Gainesville, FL 32611-6200 USA (e-mail: mohseni@ufl.edu).

Digital Object Identifier 10.1109/JSYST.2015.2487449



Fig. 1. Two examples of autonomous micro and miniature aerial vehicles in our group. Top: 60-g MAV with the wing span of 8 in and a payload capacity of 20 g [6], [7]. Bottom: 250-g miniature aerial vehicle with the wing span of 2 ft and a payload capacity of 100 g [5], [8]. All vehicles are equipped with GPS, radio, transmitter, pressure, temperature and humidity sensors, inertial measurement unit (IMU), etc.

same cost as a single large aircraft reconnaissance mission with greatly decreased risk to human life and property. This has the potential to create a paradigm shift from the use of large robust sensor platforms that can fight a hurricane's winds to small low-cost sensors that use intelligent control schemes to ride the winds. In the future, heterogeneous groups of autonomous aerial and underwater vehicles may play a key role in real-time data collection and environmental monitoring to enable higher fidelity and longer term forecasts of developing storms. MAVs can play a key role in this area.

Small aircraft systems are a very active area of research. For an overview of the topic, see [9]. However, fixed-wing MAV control strategies are scarce, mostly due to the unexplored flow regime of low aspect ratio, low Reynolds number, and low inertia [6], [10], [11].

At present, MAV and sUAS usage in hurricanes has been limited to postdisaster studies. There have been no real-world attempts to employ MAVs for *in situ* measurements within an active hurricane due to the many difficulties that must be

overcome. The most obvious limitation is the relatively low flight speed of MAVs, typically around 10 m/s, compared to hurricane winds that may exceed 70 m/s. Although larger unmanned aerial systems (UAS) have higher flight capabilities, they also represent a higher risk platform due to their higher cost and potential to cause severe damage if they crash. As a result, the operation of large UAS such as the Aerosonde platform [12] is limited to higher altitudes. On the other hand, the low cost of MAVs enables them to take on riskier tasks, flying to regions of hurricanes that have not been previously studied. Some recent research has investigated vehicle guidance in strong background flows. A few prominent examples are minimum time path planning [13], 2-D vehicle control in a Rankine vortex (motivated by control in a hurricane) [14], and nearly optimal swarm guidance in strong background flows [15], [16]. None of these published methods is easily applicable to a realistic scenario involving MAVs in a hurricane since they rely on having detailed advance knowledge of the flow field or a relatively low ratio of wind speeds to flight capabilities. New control strategies are needed. Even with improved control schemes such as the ideas presented in this paper, additional technological improvements are necessary to make this work a reality. MAVs such as those shown in Fig. 1 have limited range on the order of 20 km (at full power) relative to the background flow due to power constraints. Note that hurricane wind speeds may be quite large (up to ~ 70 m/s), so the actual distance travelled relative to the ground may be much higher. Additionally, the expectation is that, in most flights in a hurricane, next-generation MAVs may spend a significant amount of time coasting or gliding, essentially acting as passive “debris” combined with intervals of powered flight to reposition. This will increase operating time to hours and may extend the range (relative to the ground) to hundreds of kilometers.

The main purpose of this paper is to demonstrate the impact of even a very simple control scheme that is based on a high-level understanding of the hurricane dynamics. To state the obvious, a MAV with a 10-m/s flight speed cannot directly fight against the winds in a hurricane, so smarter control schemes are needed. To better understand the transport in a hurricane, we present a Lagrangian view of particle dynamics in a simulated storm using Lagrangian coherent structures (LCSs) for analysis. Based on the understanding gained from this analysis, we develop a new control scheme for MAVs in a hurricane. This control scheme is based on locating the minimum radial winds to enable flight toward the hurricane eye. Once the calm eye has been reached, MAVs can easily reposition themselves vertically or use the hurricane outflow to fly outward to any desired radius. Flight radially away from the eye is aided by the existing winds and is thus much easier and not directly addressed here. Despite the strength of the tangential winds outside the eye, MAV control in the vertical direction is still feasible [17]. A gradient descent controller is used to control the vertical position of simulated MAVs based on an estimate of the mean velocity field of a state-of-the-art high-resolution weather research and forecasting (WRF) hurricane simulation. This controller is extremely simple and computationally cheap, so it may be implemented on resource constrained MAV hardware. More intelligent controllers could be developed in the future.

We present two sets of results where the use of the gradient descent controller results in a dramatic improvement in the ability of simulated MAVs to reach the hurricane eye compared to tests using a fixed altitude controller.

II. LAGRANGIAN COHERENT STRUCTURES

Understanding weather phenomena and fluid flows in general typically requires an understanding of the transport and mixing processes involved. In a hurricane, the storm is fed by the warm moist air that is drawn inwards at the base. Energy is released as air is convected upward, and water vapor condenses into water and eventually forms ice crystals. The injected energy due to these phase changes sustains convection, which drives the inflow of additional warm moist air.

Several techniques have been developed to analyze the transport and mixing in complex fluid flows such as a hurricane. The traditional tools for analyzing dynamical systems often fail in such cases due to the aperiodic finite-time nature of complex flows. One technique that has demonstrated utility is LCS analysis. Over the past decade, LCS techniques have been used to identify the exact boundaries to vortices [18], [19], analyze pollution dispersal [20], and locate flow structures in turbulence [21], [22]. LCS applicability is far reaching and has led to new insights in many flows.

Conceptually, the idea underlying most LCS techniques is to detect regions of high Lagrangian stretching. The boundaries of coherent structures are expected to experience large stretching relative to the surrounding fluid because fluid in a coherent structure has markedly different past and future trajectories than fluid outside it. For example, a vortex ring boundary can be exactly defined by the motion of fluid particles that recirculate within the vortex compared to those that do not. This idea was primarily motivated by Haller and Yuan [21] and has since been formalized. A popular way of quantifying the stretching is to use the finite-time Lyapunov exponent (FTLE) field. The FTLE field directly measures the amount of stretching in the flow, and LCSs can then be defined as ridges (locally high values) in the FTLE field [23].

The FTLE field is computed by first computing the flow map $\Phi_{t_0}^T(\vec{x})$ for passive Lagrangian tracers in the flow

$$\Phi_{t_0}^T(\vec{x}) = \vec{x} + \int_{t_0}^{t_0+T} \vec{v}(\vec{x}^*, t) dt. \quad (1)$$

The gradient of the flow map is then computed and used to compute the deformation tensor, Δ

$$\Delta = (\nabla\Phi)^H(\nabla\Phi) \quad (2)$$

where H denotes the Hermitian transpose. Finally, λ_{\max} , the largest eigenvalue of Δ , is used to compute the FTLE values as

$$\sigma_{t_0}^T(\vec{x}) = \frac{1}{|T|} \ln \sqrt{\lambda_{\max}}. \quad (3)$$

Typically, the LCSs (the ridges of the FTLE field) are not explicitly extracted but are visualized by displaying a contour plot of the FTLE field.

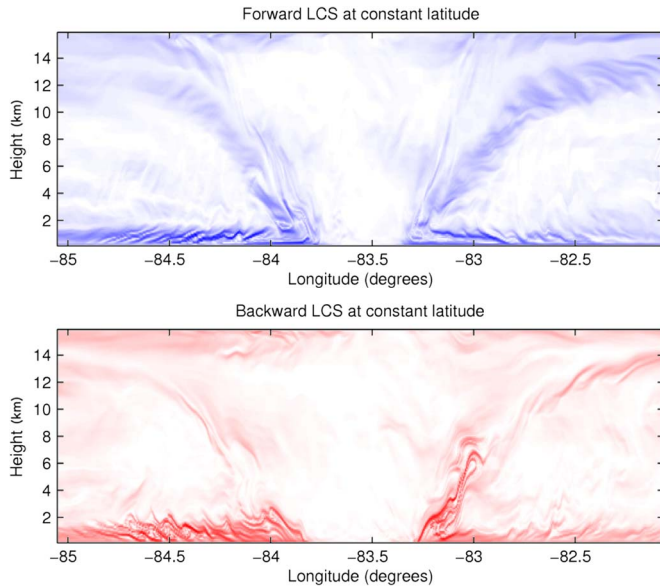


Fig. 2. Constant latitude slice of the LCS in the hurricane simulation. Top: Forward (repelling) LCS. Bottom: Backward (attracting) LCS. Darker colors indicate stronger LCS (only the relative values are important here). The calm hurricane eye is surrounded by complex and sometimes small-scale LCS. The most complex LCSs appear in the inflow region at heights less than 1 km. The observed asymmetry is due to the direction of travel of the hurricane (to the west).

In practice, LCSs reveal barriers to transport that can be used for flow and transport analysis. It is also possible to compute the forward or the backward LCS by considering either the future or past flow behavior. LCSs reveal structures that are either repelling (forward LCS) or attracting (backward LCS). For additional details, including the FTLE computation, the reader is referred to [23]. It is sufficient here to think of the backward and forward LCSs as revealing attracting or repelling regions in a flow, respectively.

A. LCS in a Simulated Hurricane

Here, LCSs are presented for a simulated hurricane in the Gulf of Mexico. The data used are from a WRF hurricane simulation of hurricane Rita (2005) provided by the National Center for Atmospheric Research (NCAR). The high resolution model has the finest grid with a 1.3-km resolution in the horizontal direction and 30-min snapshots for the data files. Although a 1.3-km grid resolution is insufficient to capture all flow scales, it is not possible to perform a fully resolved hurricane simulation with current computational resources, and this simulation is close to the state of the art and is produced by the same code used for research and forecasting by the National Weather Service. An integration time of $T = 1$ is used to compute the FTLE values.

Fig. 2 shows a constant latitude slice of the LCS for the hurricane simulation. The top part of the figure shows the repelling LCS, and the bottom shows the attracting. The LCSs reveal the complex boundary layer inflow, a calm eye bounded by LCS in the eyewall, and the upper level outflow also bounded by LCSs. The boundary layer and hurricane inflow region contains the highest wind speeds and the most complicated LCS. Friction in

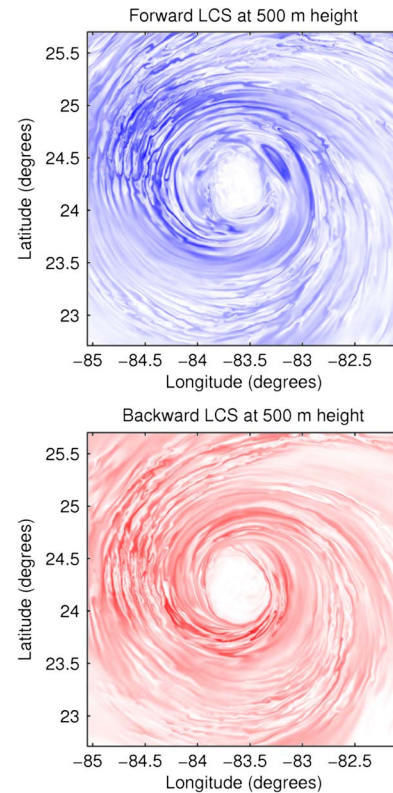


Fig. 3. 500-m altitude horizontal slice of the FTLE fields in the hurricane simulation. The top (blue) figure shows the forward LCS, revealing repelling structures. The bottom (red) figure shows the backward LCS, revealing attracting structures. Darker colors indicate stronger LCS (only the relative values are important here). Many equally strong LCSs are present in the domain, and no dominant LCS is apparent.

the boundary layer disrupts the cyclo-geostrophic balance that is present near the low pressure eye and causes radial inflow due to the existing pressure gradients (lower pressure at the center). The inflow is turned upward by convection and converging flow at the eyewall. At the same time, the hurricane has the largest wind speeds in the azimuthal direction with tangential wind speeds of more than 70 m/s, about an order of magnitude larger than the radial and vertical velocities.

As seen in Fig. 2, the LCSs outline a calm eye region, but the detailed structures surrounding the eye are too complex to be easily analyzed, particularly in the lower levels of the flow. The chaotic nature of the LCS is primarily due to the turbulence in the flow and is greatly enhanced by the prevalence of relatively small scale updrafts and downdrafts as well as high shear in the boundary layer. Fig. 3 shows a horizontal cross section of the forward and backward FTLE fields at an altitude of 500 m. The complex and highly chaotic LCSs are evident in Fig. 3, and the only major feature that is easily identified is the eye of the hurricane where no LCSs are present.

Some general trends are visible in the LCS shown in Fig. 3, including a spiral structure and a calm eye. The spiral structure and calm eye are expected and reflect the mean flow in the hurricane. However, on smaller scales, turbulence and complex flow features greatly influence particle trajectories, generating highly complex LCS. In fact, the LCSs are so complex in the boundary layer region that it is difficult to make any certain

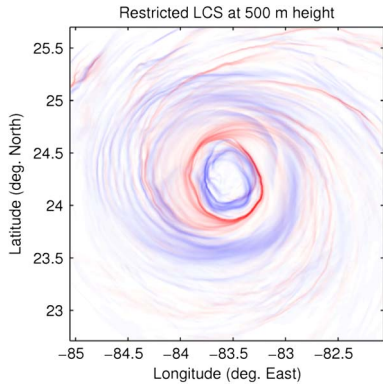


Fig. 4. 500-m altitude horizontal slice of the restricted LCS in the hurricane simulation. Both FTLE fields are shown together with the forward (repelling) LCS in blue and the backward (attracting) LCS in red. The LCSs shown here were computed in a 2-D fashion by artificially setting the vertical velocity to zero and taking finite differences only in the horizontal directions. Darker colors indicate stronger LCS (only the relative values are important here). The attracting LCS at the eyewall is the dominant feature.

statements about their quantitative effects on transport in the flow. As is often the case in turbulence, any quantitative statements will be largely based on statistics.

B. Restricted LCS

Based on the observation that the radial and vertical winds in the hurricane are about a factor of 10 less than the tangential winds, we expect that a MAV in a hurricane will have much better control over its altitude than its horizontal position. Hoping to take advantage of the background flow in a hurricane, the “restricted LCSs” are calculated for the same locations discussed earlier. For the restricted LCS, the FTLE field is computed in a 2-D fashion, artificially setting the vertical velocity to zero and taking derivatives for $\nabla\Phi$ only in the horizontal directions. These LCSs would govern the motion of particles that are restricted to horizontal movement. A horizontal slice of the restricted LCS at an altitude of 500 m is shown in Fig. 4.

The restricted LCSs reveal the key transport structures caused only by the horizontal wind field and are much simpler than the full LCS seen in Fig. 3. Additionally, a single dominant attracting (red) LCS surrounds the hurricane eye. The main attracting LCS feature is due to the converging horizontal wind field at the eyewall. At the eyewall, the inflow from outside the eye converges with slowly outflowing wind in the eyewall and turns upward to spiral up and around the eyewall. Any passive particles in the flow that are artificially restricted to a 500-m altitude and are near enough to the hurricane eyewall are observed to collect near the strongly attracting LCS.

A vertical cross section of the restricted LCS is shown in Fig. 5. It can be seen that the character of the restricted LCS sharply changes at an altitude of about 1 km, the upper limit of the hurricane boundary layer (HBL). Within the HBL, interaction with the surface generates a radial inflow that feeds the hurricane and leads to the attracting restricted LCS at the eyewall. Above the HBL, the mean radial flow component is directed away from the hurricane center, and passive particles that are artificially restricted to 2-D motion at altitudes above

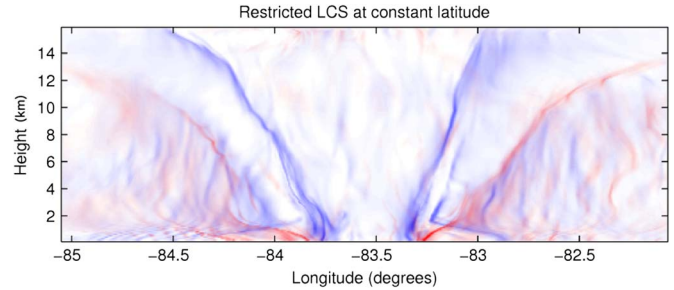


Fig. 5. Constant latitude slice of the restricted LCS in the hurricane. Darker colors indicate stronger LCS (only the relative values are important here). A transition in the LCS is seen at an altitude of ~ 1 km. Above 1-km height, the red attracting LCS at the eyewall is not present.

1 km do not collect near the eyewall, rotating around the eye or moving gradually outward instead.

III. MAV CONTROL IN STRONG BACKGROUND FLOWS

MAVs represent a small cost-effective platform for many research tasks, including environmental monitoring. MAVs may cost as little as a few hundred dollars to produce and can be outfitted with sensors to measure pressure, temperature, and humidity in addition to GPS and communication radios [6], [8], [24]. Their small size also gives a high strength relative to their mass, so MAVs do not require landing gear and are not damaged by rough landings. Similarly, high winds and turbulence may affect a MAV’s flight but cannot damage it. However, MAVs’ small size also limits their flight capabilities. A typical MAV has a maximum flight speed of around 10 m/s, much smaller than hurricane winds which may exceed 70 m/s. MAVs cannot possibly overcome such a strong wind field, so we must instead develop intelligent control schemes that take advantage of the existing transport due to the wind when possible. This represents a paradigm shift from the current methods of hurricane research which either fly against the winds with a large aircraft or offer no active sensor control.

To demonstrate the importance of smart control for MAVs in hurricanes, Fig. 6 shows the results of two preliminary simulations of MAVs flying in a high-resolution simulation of hurricane Rita (2005). In this simulation, a group of MAVs is initialized at an altitude of 550 m and a distance of 125 km from the hurricane center as shown in the top image. Flight speeds in this simulation were limited to 5 m/s to highlight an extreme case, although typical MAV speeds may be two to three times this value. In the middle image, the MAVs fly directly with the prevailing wind at a speed of 5 m/s and are quickly dispersed around the hurricane. In the bottom image, the MAVs also attempt to maintain their starting altitude by flying up or down at 5 m/s as needed. Because this 550-m altitude is in the hurricane inflow region, the MAVs are quickly drawn into the hurricane eyewall and the attracting restricted LCS seen in Fig. 4. By utilizing the existing inflow, the MAVs are able to reach the hurricane eyewall even with extremely low flight speeds.

The flight capabilities of a vehicle in a background flow can easily be quantified by the envelope of admissible flight angles. A vehicle’s flight trajectory is given by the vector sum of the vehicle’s velocity (airspeed, relative to the wind) and

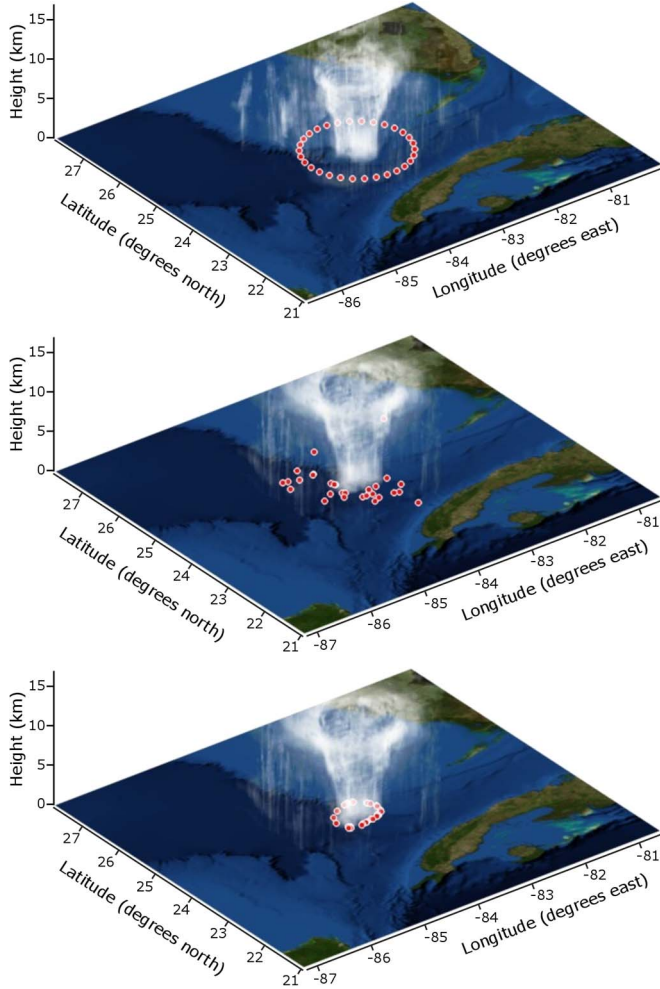


Fig. 6. Simulated MAVs placed near a high-resolution simulation of hurricane Rita. The top image shows the initial configuration of the MAVs with respect to the hurricane. The other images show the MAV positions after 104 min. The middle frame shows MAVs with no vertical control, and the bottom shows MAVs attempting to maintain a 550-m altitude. Video versions of this figure are available as supplementary material online.

the wind velocity. A realistic scenario with a MAV speed of 10 m/s and a hurricane wind speed of 70 m/s gives feasible flight angles of only $\pm 8.2^\circ$ relative to the wind. In essence, any flight plan for MAVs in a hurricane must primarily travel with the existing winds. The maneuvering capability represents only a perturbation to the background flow. Although the tangential hurricane winds may exceed 70 m/s, vertical wind speeds are typically less than 10 m/s, and the strong updrafts which may exceed 10 m/s have a very limited spatial extent. This allows MAVs a much greater degree of control over their altitude than their horizontal motion. Even if a MAV does enter a strong updraft and is displaced vertically, it will soon travel through the updraft and into regions with lower vertical wind speeds, so it is possible to reposition to the desired altitude.

Motivated by this observation, we propose the development of control schemes based on maneuvering in the vertical direction to reach regions where the winds are more favorable for the desired direction of travel within a hurricane. In this paper, we present a vertical controller for MAVs in a hurricane based on a gradient descent technique. The azimuthally averaged radial

velocity is the field of interest as the MAVs are tasked with traveling from a starting position to the hurricane center. The horizontal controller continuously guides the MAVs toward the center of the hurricane. The control scheme can be written as

$$\vec{F}_{xy} = \frac{\vec{x}_c - \vec{x}}{|\vec{x}_c - \vec{x}|}, \quad F_z = \frac{\frac{\partial \overline{U}_r}{\partial z}}{\left| \frac{\partial \overline{U}_r}{\partial z} \right|} \quad (4)$$

where \vec{F}_{xy} and F_z are vertical and horizontal control forces, \vec{x}_c is the hurricane center, \vec{x} is the vehicle position, and \overline{U}_r is the azimuthally averaged radial component of the hurricane wind field. Note that \vec{F}_{xy} is in line with the radial direction (toward the hurricane center) and no control actuation is provided in the azimuthal direction. The MAV is free to move azimuthally around the hurricane as dictated by the very strong tangential winds. This is acceptable because the hurricane is largely axisymmetric and the MAV is tasked only with reaching the center of the storm. The main purpose of the controller is to provide vertical actuation to reach an altitude of locally minimum radial wind speed (\overline{U}_r) so that the MAV has sufficient control authority (horizontal flight capabilities) to overcome the radial outflow of the hurricane. In practice, a more sophisticated low-level controller would be needed to respond to these high-level control forces.

This control scheme requires knowledge of the hurricane center and vehicle position as well as an estimate of the azimuthally averaged radial component of the wind. The hurricane center, \vec{x}_c , may be estimated from satellite images or forecasts, while \overline{U}_r must be estimated from numerical forecasts or models such as those used in hurricane track and intensity forecasting. In the future, it may be possible for a large swarm of communicating MAVs to estimate \overline{U}_r as they fly near the hurricane, but such a scheme is beyond the scope of this paper. The vertical controller attempts to position the vehicle in a region of locally smallest radial winds, which are most easily overcome in the attempt to fly toward the hurricane center in the horizontal directions. As long as a MAV is able to vertically position itself in a region where the mean radial outflow from the hurricane is less than the horizontal flight speed of the MAV, it will be able to progress toward the hurricane center. Although the azimuthal winds may be very strong, the tangential motion of the MAV is inconsequential to the control objective of reaching the hurricane center.

IV. SIMULATIONS AND RESULTS

To test the control scheme given by (4) and demonstrate its feasibility, we have performed a series of simulations based on realistic parameters for MAVs and using data from a state-of-the-art high-resolution simulation of hurricane Rita (2005). This simulation data were provided by NCAR. The hurricane has a maximum wind speed of over 80 m/s with vertical winds topping 20 m/s in the strongest updrafts.

Simulated MAVs are treated as point vehicles where the total velocity is given by the vector sum of the MAV velocity and the hurricane wind velocity. This is only a first approximation and neglects vehicle dynamics but is sufficient for the high-level analysis presented here. Linear interpolation is used in

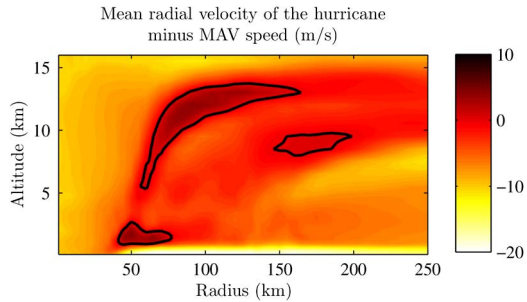


Fig. 7. Azimuthally averaged radial wind speed of the hurricane data minus the MAV speed (10 m/s). The zero contour is shown in black, and regions within this contour are infeasible for making progress toward the eye due to the large outflow velocity. Lighter colors represent regions of easier travel toward the eye. The color shows the radial velocity minus MAV speed in meters per second (see color bar for scale).

time and space to estimate the hurricane winds at the MAV locations. Inertial and vehicle dynamic effects are neglected. Lower level control algorithms are required to manage vehicle stability and gust/perturbation recovery in real-world flights. However, neglecting inertial effects for MAVs is a reasonable approximation. The small MAV shown in Fig. 1 weighs only about 60 g and would be blown around like a piece of debris in the absence of control. The MAV speed is limited to 2 m/s in the vertical direction and 10 m/s overall; these parameters reflect the capabilities of current state-of-the-art MAVs. In order to make progress toward the hurricane eye, these MAVs must fly in regions where the mean outflow velocity of the hurricane is less than 10 m/s. Regions of larger mean radial velocity are effectively occlusion regions where the MAVs should not fly. To show this, we plot the azimuthally averaged radial wind speed minus the 10 m/s MAV flight speed in Fig. 7. The occlusion regions are the darker regions within the black contour, and lighter colored regions represent feasible flight zones for the MAVs. Our gradient descent controller allows the MAVs to locate the altitudes that represent paths of least resistance between these occlusion regions, enabling flight into the hurricane eye.

For reference, we first present the result of simulations where vehicles attempt to maintain their starting altitude rather than following the gradient descent law of (4). This represents a naïve control scheme based on fixed altitude control where the success of vehicles is correlated with the mean radial velocity at their height. For each starting radius and height, a group of 100 vehicles is arrayed around the hurricane at different azimuthal locations. The simulation is run for 24 h of simulation time, and the results are shown in Fig. 8. For this fixed altitude controller, there are two altitude bands where no vehicles that start outside the hurricane eyewall are able to reach the hurricane center. This occurs in the upper level outflow region (around 12-km altitude) as well as a region from about 1–2-km height just above the HBL. These altitudes have higher mean radial wind speeds that the simulated MAVs are not able to overcome. Additionally, the lowest percentages of vehicles to reach the hurricane center are clearly those altitudes that correspond to the occlusion regions seen in Fig. 7.

We next present the results of our simulations using the gradient descent controller. For this simulation, we also note that there are certain regions of the hurricane that should be

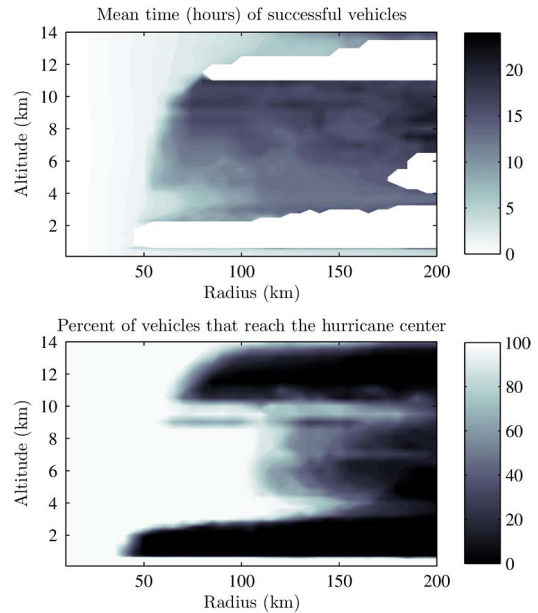


Fig. 8. Results from the naïve fixed altitude controller showing the mean time required and percent of MAVs that successfully reach the hurricane center within 24 h. The color shows the time or percentage and the position in the figure shows the vehicles' starting positions.

avoided in realistic scenarios. The lowest altitudes (below about 1 km) contain the HBL. This region is extremely turbulent and also experiences heavy precipitation in the form of rain and hail, making it extremely hazardous to vehicles. Unfortunately, avoiding this area due to the hazardous flight conditions precludes taking advantage of the strongly attracting restricted LCS seen at low altitudes near the hurricane eyewall. Additionally, the high altitude outflow region should be avoided if the vehicles are attempting to fly toward the hurricane center. This outflow also occurs well above the flight envelope of most MAVs. To avoid these regions, we set a flight window of $2.5 \text{ km} \leq z \leq 8 \text{ km}$ where vehicles outside this altitude range fly up or down until they are back in the desired range and the altitude is controlled by (4). At each time step, an estimate of $\partial \bar{U}_r / \partial z$ is determined by rounding to the nearest 30 min and computing the azimuthally averaged radial velocity field from the hurricane data. The results are shown in Fig. 9.

Compared to the naïve fixed altitude controller, the use of the gradient descent algorithm greatly improves the performance and ability of the MAVs to reach the hurricane center. At least 95% of the vehicles at each starting location reach the hurricane center within the allotted 24-h period, which is a dramatic improvement over the naïve controller. Additionally, the average time required to reach the center is decreased at all locations outside the hurricane eye.

V. CONCLUSION

Recent advances in hardware and theoretical understanding of MAVs have brought the prospect of using MAVs for hurricane research close to reality. However, the powerful winds in hurricanes, combined with their turbulent and chaotic character, make most existing control and guidance schemes infeasible.

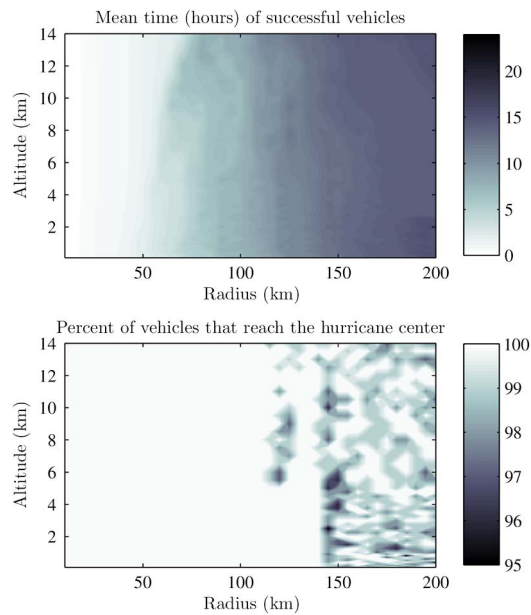


Fig. 9. Results from the gradient descent controller showing the mean time required and percent of MAVs that successfully reach the hurricane center within 24 h. The color shows the time or percentage, and the position in the figure shows the vehicles' starting positions. Note that the color scale on the bottom figure is from 95%–100%.

Feasible control schemes must account for the wind field in path planning and navigation for MAVs. Further developing and implementing such control schemes may result in a paradigm shift in mobile sensor designs for hurricane measurements where the objective is not to fight the hurricane winds but to intelligently ride the existing winds.

Despite the fact that the tangential hurricane winds may be almost an order of magnitude larger than MAV flight speeds, the vertical winds are much weaker and more spatially limited. This allows MAVs the potential to control their altitude much better than their horizontal motion, opening the possibility of altitude-based control schemes. As revealed by the restricted LCS, the horizontal transport in the investigated hurricane simulation is much simpler than the full 3-D transport. Understanding and using the horizontal winds to enable efficient navigation in and around a hurricane will enable next-generation research and data collection techniques.

We have implemented and tested a gradient descent controller for simulated MAVs in a hurricane simulation. The gradient descent controller governs the vertical motion of the simulated MAVs and guides them to local minima in the radial wind field, allowing the MAVs to progress toward the hurricane center as long as the mean radial winds are less than the MAVs' flight speed. This gradient descent controller relies on having knowledge of the MAVs' location relative to the center of the hurricane as well as the azimuthally averaged radial wind field. This radial wind field could be estimated from simulations or forecasts, or in future applications, it may be possible to estimate the wind field from direct measurements taken by a sufficient number of MAVs.

Compared to a naïve fixed altitude controller, the gradient descent controller shows a large improvement in the MAVs' ability to reach the hurricane center. At least 95% of MAVs

reach the hurricane center within 24 h regardless of their starting locations (initial radius of 0–200 km; initial height of 0–14 km). On the other hand, the naïve controller results in a large area of the domain where no vehicles are able to reach the hurricane center.

Given the limited flight capabilities of MAVs, many practical applications will require the use of efficient control algorithms to ensure mission feasibility and success. Hurricanes represent an extreme challenge in this area; the maximum wind speeds are nearly an order of magnitude larger than typical MAV flight speeds, but even in such extreme cases, some control is still feasible. The gradient descent controller presented here offers one option for guiding MAVs to a hurricane center.

ACKNOWLEDGMENT

The authors would like to thank the National Center for Atmospheric Research, particularly C. Davis and S. Fredrick, for providing access to the hurricane simulation data used in this research.

REFERENCES

- [1] "NOAA's Hurricane Hunters." accessed: 2014-02-03. [Online]. Available: <http://flightscience.noaa.gov/>
- [2] K. Moore, "Comparison Between Satellite Observed and Dropsonde Simulated Surface Sensitive Microwave Channel Observations Within and Around Hurricane Ivan," M.S. thesis, Florida State Univ., Tallahassee, FL, USA, 2012.
- [3] J. Halverson *et al.*, "Warm core structure of Hurricane Erin diagnosed from high altitude dropsondes during CAMEX-4," *J. Atmos. Sci.*, vol. 63, no. 1, pp. 309–324, Jan. 2006.
- [4] J. Franklin, M. Black, and K. Valde, "GPS dropwindsonde wind profiles in hurricanes and their operational implications," *Weather Forecast.*, vol. 18, no. 1, pp. 32–44, Feb. 2003.
- [5] J. Allred *et al.*, "SensorFlock: A mobile system of networked micro-air vehicles," in *Proc. ACM SenSys: 5th ACM Conf. Embedded Netw. Sensor Syst.*, Sydney, NSW, Australia, Nov. 6–9, 2007.
- [6] M. Shields and K. Mohseni, "Passive mitigation of roll stall for low aspect ratio wings," *Adv. Robot.*, vol. 27, no. 9, pp. 667–681, 2013.
- [7] T. Linehan, R. O'Donnell, A. Bingler, and K. Mohseni, "Modeling, control, and flight testing of a fixed-wing low aspect ratio micro-aerial vehicle," in *Proc. AIAA Guid., Navigat., Control Conf.*, San Diego, CA, USA, to be published.
- [8] A. Shaw and K. Mohseni, "A fluid dynamic based coordination of a wireless sensor network of unmanned aerial vehicles: 3-d simulation and wireless communication characterization," *IEEE Sensors J.*, vol. 11, no. 3, pp. 722–736, Mar. 2011.
- [9] R. W. Beard and T. W. McLain, *Small Unmanned Aircraft: Theory and Practice*. Princeton, NJ, USA: Princeton Univ. Press, 2012.
- [10] M. Shields and K. Mohseni, "Effects of sideslip on the aerodynamics of low-aspect-ratio low-Reynolds-number wings," *AIAA J.*, vol. 50, no. 1, pp. 85–99, Jan. 2012.
- [11] M. Shields and K. Mohseni, "Roll stall for low-aspect-ratio wings," *J. Aircraft*, vol. 50, no. 4, pp. 1060–1069, Jul. 2013.
- [12] P.-H. Lin, "Observations: The first successful typhoon eyewall-penetration reconnaissance flight mission conducted by the unmanned aerial vehicle, Aerosonde," *Bull. Amer. Meteorol. Soc.*, vol. 87, no. 11, pp. 1481–1483, Nov. 2006.
- [13] B. Rhoads, I. Mezic, and A. Poje, "Minimum time feedback control of autonomous underwater vehicles," in *Proc. IEEE CDC*, 2010, pp. 5828–5834.
- [14] L. DeVries and D. Paley, "Multivehicle control in a strong flowfield with application to hurricane sampling," *J. Guid., Control, Dyn.*, vol. 35, no. 3, pp. 794–806, May 2012.
- [15] D. Lipinski and K. Mohseni, "A master-slave fluid cooperative control algorithm for optimal trajectory planning," in *IEEE Int. Conf. Robot. Autom.*, Shanghai, China, May 9–13, 2011, pp. 3347–3351.

- [16] D. Lipinski and K. Mohseni, "Nearly fuel-optimal trajectories for vehicle swarms in open domains with strong background flows," in *Proc. IEEE/RSJ Int. Conf. IROS*, Tokyo, Japan, Nov. 3–7, 2013, pp. 3837–3842.
- [17] D. Lipinski and K. Mohseni, "Feasible area coverage of a hurricane using micro-aerial vehicles," presented at the AIAA Scitech, National Harbor, MD, USA, Jan. 13–17, 2014, Paper 2014-0894.
- [18] S. Shadden, J. Dabiri, and J. Marsden, "Lagrangian analysis of fluid transport in empirical vortex ring flows," *Phys. Fluids*, vol. 18, no. 4, pp. 7105–7120, Apr. 2006.
- [19] D. Lipinski and K. Mohseni, "A numerical investigation of flow structures and fluid transport with applications to feeding for the hydromedusae *Aequorea victoria* and *Sarsia tubulosa*," *J. Exp. Biol.*, vol. 212, no. 16, pp. 2656–2667, Sep. 2009.
- [20] C. Coulliette, F. Lekien, G. Haller, J. Paduan, and J. Marsden, "Optimal pollution mitigation in Monterey Bay based on coastal radar data and nonlinear dynamics," *Environ. Sci. Technol.*, vol. 41, no. 18, pp. 6562–6572, Aug. 2007.
- [21] G. Haller and G. Yuan, "Lagrangian coherent structures and mixing in two dimensional turbulence," *Phys. D, Nonlinear Phenom.*, vol. 147, no. 3/4, pp. 352–370, Dec. 2000.
- [22] M. Green, C. Rowley, and G. Haller, "Detection of Lagrangian coherent structures in 3d turbulence," *J. Fluid Mech.*, vol. 572, pp. 111–120, Feb. 2007.
- [23] S. Shadden, F. Lekien, and J. Marsden, "Definition and properties of Lagrangian coherent structures from finite time Lyapunov exponents in two-dimensional aperiodic flows," *Phys. D, Nonlinear Phenom.*, vol. 212, no. 3/4, pp. 271–304, Dec. 2005.
- [24] J. Hall and K. Mohseni, "Micro aerial vehicles," in *Encyclopedia of Microfluidics and Nanofluidics*, D. Li, Ed. New York, NY, USA: Springer-Verlag, 2008, pp. 1103–1110.



Doug Lipinski received the Ph.D. degree in applied mathematics from the University of Colorado at Boulder, Boulder, CO, USA, in 2012.

He worked as a Postdoctoral Researcher in the Department of Mechanical and Aerospace Engineering at the University of Florida, Gainesville, FL, USA, from 2012 to 2014. He is currently working as a member of the technical staff at Massachusetts Institute of Technology Lincoln Laboratory.



Kamran Mohseni (M'95) received the Ph.D. degree in mechanical engineering from the California Institute of Technology (Caltech), Pasadena, CA, USA, in 2000.

After a year as a postdoc in control and dynamical systems at Caltech, he joined the University of Colorado at Boulder, Boulder, CO, USA, as an Assistant and then Associate Professor in Aerospace Engineering Sciences before moving to Florida as the W.P. Bushnell Endowed Chair in both the Mechanical and Aerospace Engineering Department and

the Electrical and Computer Engineering Department at the University of Florida, Gainesville, FL, USA. He is the Director of the Institute for Networked Autonomous Systems.

Dr. Mohseni is a member of the American Society of Mechanical Engineers, the American Physical Society, and the Society for Industrial and Applied Mathematics and an associate fellow of the American Institute of Aeronautics and Astronautics.